

Introducing a new specimen shape to assess the fatigue performance of asphalt mastic by dynamic shear rheometer testing

Markus Hospodka · Bernhard Hofko  · Ronald Blab

Received: 13 December 2017 / Accepted: 5 March 2018
© The Author(s) 2018

Abstract Early failure of asphalt pavements is a common issue all around the world. Damages are caused by various reasons like insufficient binder or aggregate quality, an inadequate mix design or improper handling in the production/construction process. The effects of binder, aggregates and mix design have been widely studied and state-of-the-art testing methods are available for both, hot-mix asphalt (HMA) and for each component. An important part in HMA belongs to the asphalt mastic, where no standardized method is available to allow a quality control. Asphalt mastic is the mix of bitumen with aggregates smaller than 63 (125) μm and covers the coarse aggregates as the actual binding component in the mix. This research aims at developing a testing method for asphalt mastic based on fatigue tests. The dynamic shear rheometer (DSR) was found as a suitable device for this purpose. The DSR fatigue test consists of the 8 mm parallel-plate geometry widely used for binder performance grading with a sample height of 3 mm. Instead of a cylindrical specimen shape, a hyperboloid of one sheet is applied. This shape predetermines the point of failure and prevents adhesion/interface failures between the mastic specimen and the upper or lower DSR stainless steel plate.

The specimens are prepared directly in the DSR employing a silicone mould to ensure an exact specimen shape. This test can be applied to all DSR devices without costly changes or additional equipment as long as sufficient cooling capacity and torque can be provided from the DSR. This fatigue test makes it possible to assess the fatigue performance of binders and mastic samples.

Keywords Mastic · Filler · Fines · Fatigue · DSR

1 Introduction

In recent years, damage has increasingly occurred in the case of bituminous surface layers, such as the loss of aggregates and decreased fatigue life of the base layers in various parts of Central and Western Europe. These damages cannot be attributed either to a severe weather phenomena or a dramatically increased traffic load. A possible cause of damage is a lack of quality of the asphalt mastic (bitumen + mineral fine fraction), like poor adhesion to the aggregates or overall lack in strength. This can be due to poor quality of one of the two components, bitumen and added filler or fines, respectively. Preliminary work [1–3] on this subject suggests that the mineralogical composition of the added filler or fines affects the quality of the mastic and thus the adhesion to the coarse aggregates and

M. Hospodka · B. Hofko (✉) · R. Blab
Institute of Transportation, Vienna University of
Technology, Gusshausstrasse 28/E230-3, 1040 Vienna,
Austria
e-mail: bernhard.hofko@tuwien.ac.at

strength. It can be assumed that a lack of quality of the added filler or fines is responsible for premature damage. Possibly, the use of non-quality-assured fines from the fine and coarse aggregates instead of added filler or mixed filler can be accounted to these damages. This study aims to develop a suitable test to assess the quality of asphalt mastic with regard to durability (fatigue life).

The European Standard EN 12697-24 [4] defines fatigue as “...the reduction of strength of material under repeated loading when compared to the strength of a single load”. Fatigue is the progressive and localized structural damage that occurs when a material is subjected to cyclic loading below the stress limit until the state of serviceability limit or total failure is reached.

This effect also occurs in asphalt pavements and affects all asphalt layers. Due to continuous heavy goods vehicle (HGV) traffic tensile stress occurs in the base layer and thus micro-cracks accumulate. In the case of repeated loads, these cracks are propagated upwards and are linked to macro-cracks, which are visible. If these cracks finally pass through to the top layer, a cracking pattern typical of fatigue damage occurs. Another form of fatigue damage affects the asphalt surface. The coarse aggregates are held together by asphalt mastic and under repeated (shear) stresses, poor mastic leads to loss of aggregates on the surface. While there are standardized testing methods available for bitumen, aggregates and hot-mix asphalt (HMA), there is no testing method available to assess the durability of asphalt mastic. Thus, several researchers already published their work to account the fatigue performance of asphalt mastic or mortar (bitumen + filler + sand) in different testing setups and machines, like DSR [2], Annular Shear Rheometer (ASR) [5–8], Dynamic Mechanical Analysis (DMA) [9–11] and Tension Compression Tests [12, 13]. All of these tests are based on applying dynamic loads (shear or tension–compression) onto bitumen, mastic or mortar specimens with different shape at different temperatures, frequencies and loading modes. Table 1 gives an overview of published work, applied setups and testing parameters for DSR and DMA. DMA consists of a DSR with special clamping system instead of parallel-plate or plate and cone geometries.

2 Approach and objectives

The 4-Point Bending-Beam Test (4PBB) according to EN 12697-24 [4] is one of the standardized fatigue tests for HMA. Since the aim of this paper is the development of a fatigue test for asphalt mastic, the 4PBB test is described in more detail for a better understanding of fatigue. In the 4PBB test, a prismatic beam is supported at 4 points and is dynamically loaded at the two inner bearings. The sample is pulled upwards and pushed downwards until a defined deformation/strain is reached in the centre of the beam. The force required for the predetermined strain is measured and the dynamic modulus is calculated continuously. Therefore, the 4PBB test is a so called strain-controlled test. Due to the increasing number of load cycles during the test progress the beam becomes weaker and the dynamic modulus is getting lower. As soon as the dynamic modulus reaches half of its initial value at the beginning of the 4PBB test the fatigue criterion is met. Tests have to be carried out at 3 different strain levels with at least 6 samples each level to maintain a limited statistic certainty. This results in at least 18 samples that have to be tested. Including the mixing of HMA, sample fabrication and preparation for testing, it takes about 3 weeks to complete all necessary steps for one single HMA. Thus, the 4PBB test is a time consuming test and it is also not applicable to the testing of asphalt mastic or mortar.

This paper aims to find a fatigue testing method suitable for asphalt mastic applicable on a device that is already available in most of the commercial laboratories of pavement engineering. The dynamic shear rheometer (DSR) was found as a suitable device with good availability due to the fact that it is used for binder grading. The objectives of this paper are:

- Development of a fatigue test with new specimen geometry applicable to all standard DSR setups used for binder grading.
- Study into test repeatability.
- Assess the fatigue performance of asphalt mastic with particle size < 125 μm .



Table 1 Publications of dynamic tests for bitumen, mastic and mortar

| References | Device | Material | Specimen geometry (mm) | Loading mode | Temperature (°C) | Frequency (Hz) |
|-----------------------|-------------|--------------------|---|------------------------|--------------------------------|------------------|
| Ameri et al. [14] | DSR | Bitumen | PP08/2 ^a | CD ^c | 25 | 10 |
| Mukandila et al. [15] | DMA | Bitumen | Column ($\varnothing 20$, $h = 20$) | CD | 0–25 | 10 |
| Shan et al. [16] | DSR | Bitumen | PP08/2 | CD and CS ^c | 20 and 25 | 10 |
| Santagata et al. [17] | DSR | Bitumen | PP08/2 | CS | 10 and 20 | 10 |
| Liao et al. [18] | DSR | Mastic | PP08/2 | CD | 20 | 10 |
| Hintz et al. [19] | DSR | Bitumen | PP08/2 | CD | 10–30 (iso ^d) | 10 |
| Stimilli et al. [20] | DSR | Bitumen | PP08/2 | CD | 19–34 (iso) | 10 |
| Mo et al. [21] | DMA | Mortar | Column ($\varnothing 6$, $h = 20$) | CS | 0 and 10 | 10 and 40 |
| Liao et al. [22] | DSR | Mastic | PP08/2 | CS | 20 | 10 |
| Soenen et al. [23] | DSR | Bitumen | PP08/2 | CD | 6–26 (iso) | 25 |
| Shen et al. [24] | DSR | Bitumen and mastic | PP08/2 | CD | 12 | 20 |
| Shan et al. [25] | DSR | Bitumen | PP08/2 | CD and CS | 25 | 10 |
| Ortiz et al. [26] | DSR | Bitumen | PP08/2 | CD | 20 | 1.59 |
| Liu et al. [27] | DSR and DMA | Bitumen and mortar | CP08/2 ^b column ($\varnothing 6$, $h = 20$) | CD | 10 | 10 |
| Shen et al. [28] | DSR | Bitumen | PP08/2 | CS | 15 and 20 | 10 |
| Shan et al. [29] | DSR | Bitumen | PP08/2 | CS | 20 and 25 | 10 |
| Martono et al. [3] | DSR and DMA | Bitumen and mastic | PP08/2 column ($\varnothing 12$, $h = 30$) | CS | 10 and 25 | 10 |
| Planche et al. [30] | DSR | Bitumen | PP08/2 | CD | $ G^*_{iso} = 5$ and 45 MPa | 10 |
| Kim et al. [2] | DSR | Bitumen and mastic | PP08/2 | CD | 25 | 10 |
| Bonnetti et al. [31] | DSR | Bitumen | PP08/2 | CD and CS | $ G^*_{iso} = 15$ MPa | 1.59 and 10 |
| Anderson et al. [32] | DSR | Bitumen | PP08/1,2,3 | CD | – 4–12, $ G^*_{iso} = 15$ MPa | 10 |
| Smith et al. [1] | DSR | Bitumen and mastic | PP08/2 | CD | 10 | 40 |
| Bahia et al. [33] | DSR | Bitumen | PP08/2 | CD | $ G^*_{iso} = 0.002$ –2 MPa | 0.15, 1.5 and 15 |

^aParallel-plate geometry, 8 mm diameter, 2 mm specimen height

^bCone and plate geometry, 8 mm diameter, 2 mm thickness of the edge film

^cControlled stress (CS), controlled strain (CD)

^dIso-stiffness temperature

3 Development of the fatigue test

3.1 DSR loading mode and fatigue failure criterion

DSR are capable of applying oscillatory stress- and strain-controlled loads on small specimens. Deciding between stress- and strain-controlled loading modes, the stress-controlled mode is in favour because it is more comparable to what happens on site. Taking a HGV passing an asphalt pavement into account, the induced stress is independent, while the strain is a function of the stiffness of the material. Under strain-controlled loading mode stiffer materials are subjected to higher stress levels than materials with lower stiffness. Changing the loading mode also requires changing the fatigue criterion. While 50% of the initial modulus is used as a criterion for strain-controlled tests, the true failure of the specimen is applied to stress-controlled tests. Figure 1 shows a typical fatigue curve under stress-controlled loading mode obtained by DSR within this paper.

A fatigue curve obtained by stress-controlled testing consists of four typical phases: Phase (1) is the adaption phase dominated by thixotropy [25, 29] and limited heating of the specimen caused by energy dissipation (both causes a reversible loss of stiffness). Phase (2) consist of a continuous propagation of micro-cracks. In Phase (3) these micro-cracks are

linked to macro-cracks until in Phase (4) these macro-cracks are linked to a yield line. Finally, the specimen breaks due to fatigue failure. The failure is reflected in both, dynamic modulus and phase lag. In this study, the point of failure is determined by the sudden drop of the phase lag (δ_{\max}) as shown in Fig. 1. However, there are several other fatigue failure criteria such as 50% reduction in stiffness or Rowe's criteria based on changes in dissipated energy. The fatigue tests are carried out in one single go without rest periods. Thus, healing effects are not accounted in this study. Healing effects are well known in literature and are depending on binder grading, temperature and applied stress or strain level [20, 28, 29, 32].

3.2 Issues and challenges with the DSR

During the development of the fatigue test three different DSR were in use for different reasons. These reasons can be accounted to the testing geometry and cooling capacity/efficiency and have to be described in detail because of the huge impact to the fatigue test:

1. Thermo Scientific HAAKE MARSII Modular Rheometer.
2. Anton Paar MCR300 Smartpave series with active Peltier-temperature-controlled sample hood (H-PTD120).

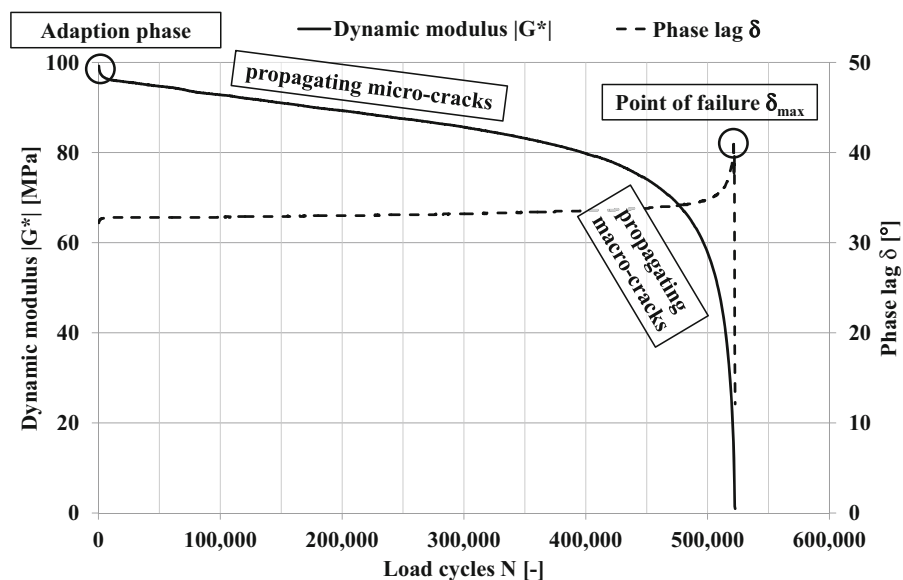


Fig. 1 Fatigue curve under stress-controlled loading mode



3. Anton Paar MCR302 with active Peltier-temperature-controlled sample hood and optional air flushing (H-PTD200).

Asphalt mastic or mortar is about 3–6 times stiffer than the neat binder. The stiffness is mainly dependent on the amount of aggregates (filler, fines) mixed with the binder but also the mineralogy, grading curve, grain shape and surface characteristics play an important role. The first DSR, a HAAKE MARSII has been employed for preliminary tests and was further proposed for all tests within this study. But this specific DSR is not suitable for fatigue tests for two reasons: First, the testing geometries are mounted with a thread and they get loose during long-term tests with stiff materials at high frequencies (Fig. 2a). Second, the drive engine is capable of enough torque but it is not durable and fails with an engine overheat error after about 10 to 30 min depending on the pre-set stress. The second DSR, a MCR300 is both, durable without any overheating issues and testing geometries are mounted with a patented mechanical coupling called QuickConnect. A MCR300 Smartpave series is equipped with a Peltier-temperature-controlled hood and testing geometries with a hollow plastic cylinder and a disposable measuring plate (Fig. 2b). While the plastic cylinder serves as a thermal barrier to the upper steel shaft, the disposable plate is used to measure curing materials like epoxy glue. The disposable plate is equipped with a thread used to fix the plate on the plastic cylinder. The adhesive used to fix the plate onto the cylinder was in focus because of its compliance at testing conditions. The disposable plate got even loose after some fatigue tests. Thus, it was necessary to apply a 2-component adhesive to fix the plate onto the plastic cylinder. Most of the fatigue tests have been carried out on this device until it became defective. Because of a discontinued support of this 15 year old DSR, there was no opportunity to get it back to a working state. During the fatigue tests on the old

MCR300 a new MCR302 became available to the lab. In comparison to the MCR300 Smartpave series, the MCR302 is equipped with a stronger Peltier-temperature-controlled hood with optional air flushing. Preliminary tests on the new MCR302 have been carried out without additional air flushing. Due to the fact that the new testing geometries have no thermal barrier included (Fig. 2c) it is necessary to switch on the air flushing of the hood (200 L_n/h). The perfusing air is efficiently cooled down to target temperature of + 10 °C. Without air flushing there is a thermal gradient from the bottom plate to the testing geometry causing a lower initial dynamic modulus at the beginning of the fatigue test in comparison to the dynamic modulus obtained by the MCR300. This thermal gradient has also been confirmed by measuring the temperature with tiny thermocouples (Type K) inside a loaded sample showing about + 15 °C at the top interface from sample to testing geometry.

Fatigue testing was continued after a homogeneous temperature distribution was ensured within the whole sample. These resulted in the same initial dynamic modulus for every mastic sample as obtained by the old MCR300. Expecting the same fatigue life (number of load cycles until failure), samples tested in the new MCR302 show a 1.5–2 times higher fatigue life and a better repeatability. While at least six fatigue tests were necessary to obtain a limited statistical certainty for the MCR300, three tests are sufficient for the MCR302. These phenomena are related to the dissipated energy into the sample causing local heating due to friction and the different cooling efficiency of the sample hoods of both devices. The cooling efficiency of the sample hood with air flushing of the MCR302 is higher than of the MCR300. During controlled-stress testing mode, heating leads to lower stiffness causing higher strain rates and shorter fatigue life. The improved repeatability can be accounted to a more homogeneous temperature distribution within the sample and complete removal of any side effects

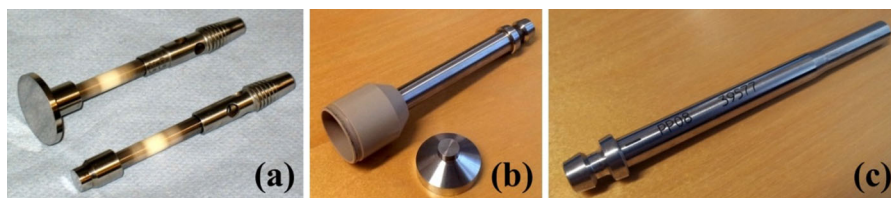


Fig. 2 Testing geometries from **a** HAAKE MARSII, **b** MCR300 and **c** MCR302

from the outside (e.g. room temperature, airflow caused by room ventilation) due to the more efficient sample hood of the MCR300. It must be noted that fatigue tests in DSR have a very high sensitivity to the sample cooling, and fatigue response is highly depending on the test temperature. Standardized binder grading is not affected of this phenomenon because of the test requirements: First, because of the low frequency (1.592 vs. 30 Hz) and second, there is no need for continuous oscillation during stepwise temperature sweeps.

3.3 Preparation of asphalt mastic samples

Depending on aggregate gradation, air void and binder content, HMA is categorized into asphalt concrete (AC), stone mastic asphalt (SMA), mastic asphalt (MA) and porous asphalt (PA). The ratio of binder to filler or fines is different within these mix designs. A mixing ratio of 1 part binder to 1.5 parts of filler or fines by weight (m/m) is chosen to obtain a ratio almost similar to the ratio used in AC. In preliminary tests mixing ratios of up to 1:2.5 have been tested where rations from 1:2.0 show a decreasing repeatability. This can either be accounted to bad mixing quality or the grain shape. The higher the content of filler or fines the higher is the interaction level between each single grain. The higher the interaction level the more prone is a poured DSR specimen to the exact position of each grain. Both, the filler or fines and the binder are heated up to +180 °C in a thermal chamber. The next step is to pour the binder into the metal can with the filler/fines inside and it is then stirred with a metal or glass rod until a homogeneous asphalt mastic sample is obtained. A temperature controlled heat gun is used to maintain the temperature during mixing. Stirring is continued during the cooling down period as long as it is possible to mix. The mastic samples are then immediately stored in a refrigerator at +5 °C to avoid settling of particles after mixing. Two different fillers (limestone and quartzite) have been tested in this study, both of them with a maximum grain size of 125 µm. It is important to keep a certain maximum grain size when comparing fillers or fines because of the sensitivity to fatigue tests. As a binder a 70/100 paving grade bitumen with a PG 64-22 (continuous PG 65-25) is used. The performance grade (PG) was obtained by DSR (EN 14770 [34]) and BBR (EN 14771 [35]) and the binder

is graded according to AASHTO M 320 [36]. Table 2 shows the binder properties at three different ageing levels (virgin, RTFOT and RTFOT + PAV) in terms of needle penetration (EN 1426 [37]), softening point ring and ball (EN 1427 [38]) and breaking point Fraass (EN 12593 [39]), respectively. It is known from literature that the stiffness of a binder has an impact to the fatigue life of the asphalt mastic [19, 20, 23, 30–33]. Due to the fact that only one binder is used in this paper this behaviour is not further accounted. However, different binders are part of the ongoing project. For the comparison of different binder grades it is necessary to perform the fatigue tests either at equi-viscous temperature or at several temperatures. The latter could make it possible to calculate life cycle costs based on fatigue life for a specific climate on site.

3.4 Test parameters and sample geometry

While a temperature sweep is applied during binder grading the fatigue test is carried out at one single temperature only. The temperature is selected according to the creep stiffness of the mastic. The higher the creep stiffness is, the higher the applicable temperature can be chosen for the fatigue test. It is necessary to maintain a certain minimum stiffness at test temperature to avoid creep deformation [32]. In this study and in accordance to other researchers a test temperature of +10 °C is selected (see Table 1). Fatigue performance testing requires a high number of load cycles until fatigue failure. It is recommended to select a high frequency to conduct these tests in a limited time to be economical. For that reason a testing frequency of 30 Hz is selected in this study. With 30 Hz it is possible to perform 108,000 load cycles within 1 h. It is possible to choose even higher frequencies as far as an appropriate DSR is available. However, higher frequencies cause higher dissipated energy and thus, more friction heating to the mastic sample.

There are two different parallel-plate testing geometries used for binder grading, PP08 and PP25. The numbers determine the diameter of the specimen and are applied to the upper (PP25) and lower temperature testing range (PP08) according to AASHTO M 320 [36]. Due to the fact that bitumen is a highly temperature-dependent material and DSR are limited in its applicable torque, PP08 has to be used for fatigue testing. In preliminary tests the standard

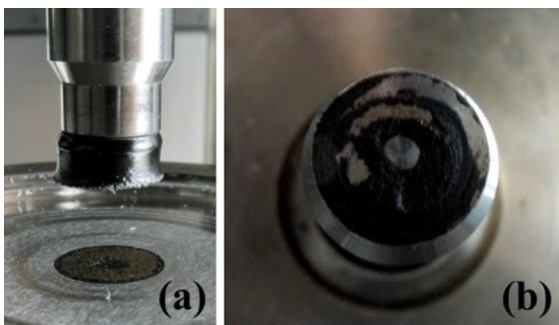
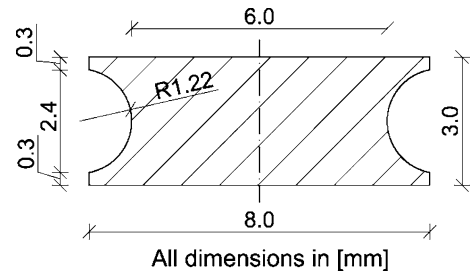


Table 2 Binder properties

| Ageing level | Penetration (0.1 mm) | Softening point (°C) | Breaking point (°C) |
|--------------|----------------------|----------------------|---------------------|
| Virgin | 80 | 45.2 | - 19 |
| RTFOT | 50 | 52.2 | - 15 |
| RTFOT + PAV | 25 | 56.2 | - 8 |

specimen geometry shape (diameter 8 mm, height 2 mm) used for binder grading have also been used for fatigue tests. After extensive pre-tests, it can be concluded that a cylindrical specimen shape (even with a height of 3 mm) is not suitable for fatigue testing due to the fracture behaviour. In all these tests performed, the specimens failed either as pure interfacial/adhesion failure (Fig. 3a) or in a combination of adhesion and cohesion failure (Fig. 3b). However, several researchers published their work employing a cylindrical specimen shape for fatigue testing of pure binder or mastic [14, 16, 18, 20, 22–25, 28–32]. Some researchers came to the same conclusion regarding the disadvantageous use of a cylindrical specimen shape for fatigue testing [15, 21].

A solution has been found in a redesigned specimen geometry (Fig. 4). This geometry is based on the PP08 testing geometry with a specimen height of 3 mm and a predetermined point of failure in the middle of the height. Higher specimens are not recommended due to the limited cooling capacity of the DSR (thermal gradient). The predetermination is realised by circular necking of the original diameter of 8 mm down to 6 mm. A small platform of 0.3 mm at both ends of the hyperboloid avoids unfavourable stress concentrations in the edges. In literature, researchers solved that issue with other specimen shapes like dog-bone or even larger cylinders with clamps or terminals at both ends [15, 21, 27]. These specimen shapes requires a DSR

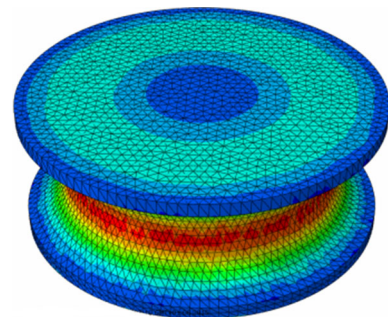
**Fig. 3** a Pure adhesion/interface failure, b partial adhesion/cohesion failure**Fig. 4** Hyperbolic specimen shape

with a temperature-controlled chamber instead of a temperature-controlled hood. This leads to expensive, additional equipment not usual or even not available for standard DSR setups employed for binder grading.

Figure 5 shows the shear stress distribution in the hyperboloid where the stress goes from higher (red) to lower levels (blue), calculated by finite element analysis software Abaqus. With this geometry it is possible to obtain true cohesion failure within the mastic specimen.

3.5 Specimen preparation in the DSR

The specimen preparation has to be carried out directly in the DSR because it is not possible to trim a hyperbolic shape by hand. A reusable silicone mould is employed to ensure an accurate specimen. The silicone mould is made out of two-component silicone and is temperature-resistant of up to + 180 °C. Thus,

**Fig. 5** FE model of the hyperbolic specimen shape

it is possible to pour the molten mastic sample directly into the silicone mould loaded in the DSR. The loading of molten samples guarantees an ideal bonding between mastic and the smooth stainless steel surfaces of the DSR. It is optional to remove excess mastic at the top of the mould because it has no impact to the fatigue test. The silicone mould is removed after a cooling period of at least 10 min resulting in an accurate specimen shape (Fig. 6a). The fatigue test starts after another cooling period of 15 min to achieve thermal equilibrium and lasts until the total failure of the specimen (Fig. 6b).

4 Results

4.1 Hyperboloid: a challenging specimen shape

It must be noted that the dynamic modulus calculated by the DSR software (Anton Paar RheoCompass) is not the true dynamic modulus of the mastic sample being measured. This issue is related to the hyperbolic specimen shape. Parallel-plate tests are usually run with cylindrical specimen shapes and therefore, all the calculations within the DSR software are based on a cylindrical shape with a diameter of 8 mm and a sample height of 3 mm. Equalling $\varnothing 6$ and $\varnothing 8$ mm for shear stress (Eq. 1) and shear strain (Eq. 2) gives a correction factor for the dynamic modulus of 3.2 (Eq. 3). Hence, a cylindrical specimen with $\varnothing 8$ mm is expected to be 3.2 times higher in dynamic modulus than a cylindrical specimen with $\varnothing 6$ mm.

$$\tau : \frac{2 \cdot M_{8\text{mm}}}{\pi \cdot r_{8\text{mm}}^3} \cdot f_{\text{korr.}\tau} = \frac{2 \cdot M_{6\text{mm}}}{\pi \cdot r_{6\text{mm}}^3} \quad (1)$$

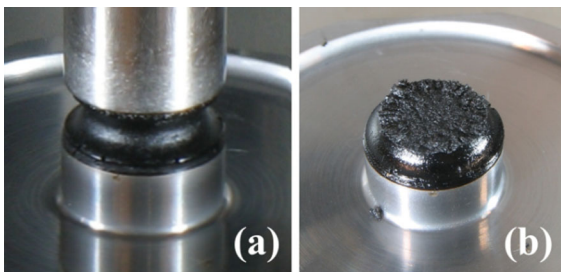


Fig. 6 a Loaded DSR specimen, b specimen after fatigue test



$$\gamma : \frac{\alpha_{8\text{mm}} \cdot r_{8\text{mm}}}{h_{8\text{mm}}} \cdot f_{\text{korr.}\gamma} = \frac{\alpha_{6\text{mm}} \cdot r_{6\text{mm}}}{h_{6\text{mm}}} \quad (2)$$

$$|G^*| : f_{\text{korr.}|G^*|} = \frac{\tau}{\gamma} = \frac{f_{\text{korr.}\tau}}{f_{\text{korr.}\gamma}} \quad (3)$$

where $|G^*|$ dynamic modulus [Pa], α deflection angle [rad], τ shears stress [Pa], h specimen height [m], γ shear strain [-], $f_{\text{korr.}\tau}$ correction factor τ , M maximum torque $f_{\text{korr.}\gamma}$ correction factor γ , r radius testing geometry [m], $f_{\text{korr.}|G^*|}$ correction factor $|G^*|$.

Oscillatory shear tests on a bitumen 70/100 with the same conditions as applied for the fatigue tests (+ 10 °C, 30 Hz sample height of 3 mm) on both, $\varnothing 8$ mm cylindrical and hyperbolic shape resulted in a correction factor of 2.4. This means that the dynamic modulus of the $\varnothing 8$ mm cylindrical specimen is not as high as expected from calculations or vice versa, the hyperboloid is stiffer than expected. It is highly likely that the contributing diameter or volume of the hyperboloid is higher than 6 mm because of the circular necking. Probably, this correction factor is varying depending on the grading curve and grain shape of the filler/fines as well as the grading or (polymer-) modification of the binder. This issue is shown in Fig. 7 and will be looked into in future work.

4.2 Repeatability of the developed fatigue test

Tests are required to have a good repeatability and comparability to guarantee a wide spread application. Figure 8 shows the repeatability of 10 fatigue tests at a shear stress level of 400 kPa of both, dynamic modulus at the beginning of each fatigue test and the fatigue life expressed as the number of load cycles until failure. The dynamic modulus is obtained after 10 s, which is equal to 300 load cycles. While EN 14770 [34] for standard DSR tests pre-sets the comparability of the dynamic modulus to 10%, there is no value given for the repeatability. It has to be accounted that this comparability is based on a round-robin test with a cylindrical specimen shape. Because there is no repeatability given, the mean $\pm 5\%$ is shown in Fig. 8. The 50% (median) and 95% confidence interval of the standard error (SEM) is calculated to look into the quality of the obtained fatigue life. With a probability of 95% the true fatigue life is between 188,000 and 212,000 load cycles. This is about $\pm 6\%$ of the mean. It can be seen that both,

Fig. 7 Contributing diameter or volume of cylindrical and hyperbolic specimen shape

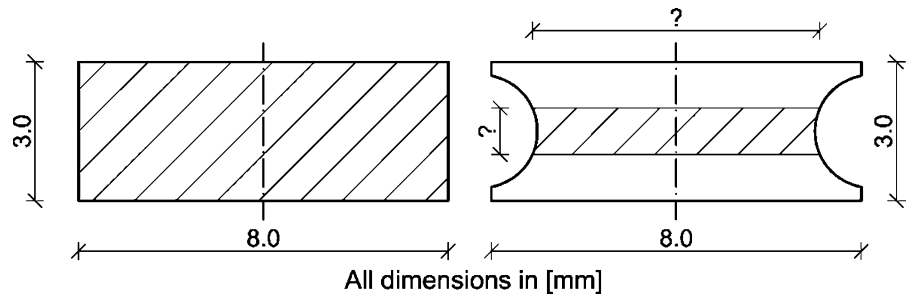
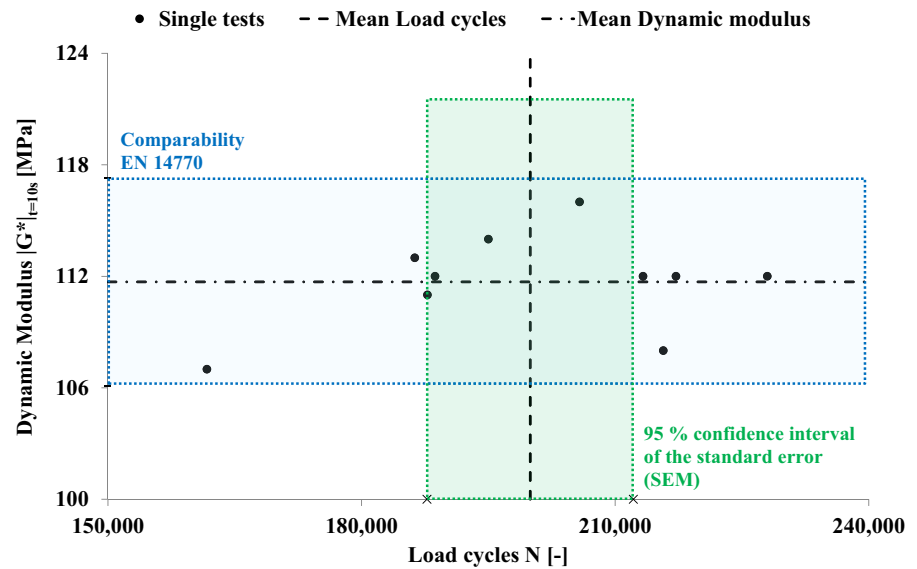


Fig. 8 Repeatability test with hyperbolic shape at + 10 °C and 400 kPa



dynamic modulus and fatigue life show a good repeatability. This proves that the hyperboloid specimen shape can be prepared very accurately and the entire DSR setup is suitable for fatigue testing.

4.3 Comparison of mastic samples

For the determination of the fatigue life of a mastic sample and for the comparison to other samples it is necessary to fit a logarithmic stress-cycle ($S-N$) curve (Wöhler curve) into the fatigue test results obtained of at least three different shear stress levels. Figure 9 shows $S-N$ curves of two different mastic samples, both mixed with the same 70/100 paving grade bitumen and mixing ratio 1 part bitumen to 1.5 parts filler by mass. Both curves are fitted to the mean values of three single fatigue tests at four different shear stress levels, respectively. Both $S-N$ curves show an excellent coefficient of determination of $R^2 = 0.99$. The performance of limestone seems to be far superior

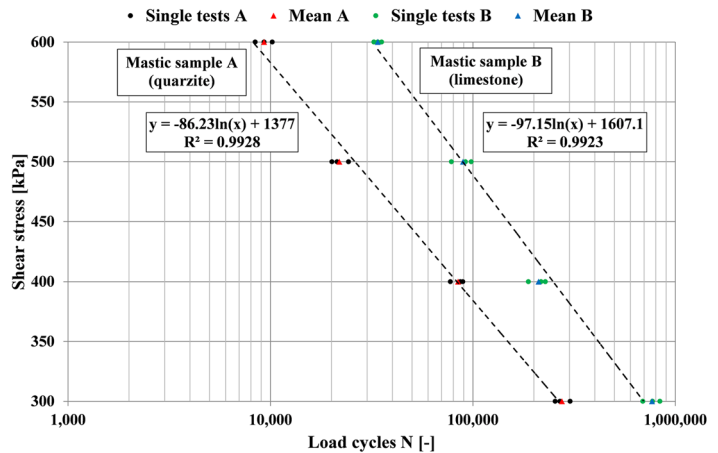
that for quartzite, but it has to be noted that the grading curve [1] and the density (filler volume concentration [22]) have an high impact on the fatigue performance and is not accounted in this study.

5 Conclusions and outlook

5.1 Conclusions

This study shows that a standard DSR equipped with components used for binder grading (temperature-controlled hood, PP08 geometry) is capable of fatigue testing of asphalt mastic. Therefore, no costly changes are necessary. The developed hyperbolic specimen shape with predetermined point of failure gives a good repeatability. This makes it possible to compare the fatigue durability of different mastic samples with $S-N$ curves at different shear stress levels. However, the hyperbolic shape is challenging in terms of the

Fig. 9 S – N curves of two different asphalt mastic samples



calculation of the true dynamic modulus compared to a cylindrical specimen shape.

5.2 Outlook

This paper is limited to one binder and two different fillers. Further tests with different binders and filler/fines are still ongoing. Another aim of this project is to determine the impact of different temperatures on the fatigue life of mastic. As soon as the fatigue life of several fillers/fines is found, a correlation analysis with 4PBB results will be carried out. The actual state of the developed fatigue test does not allow any kind of weathering. Because fillers/fines can have high water susceptibility, it is important to find a suitable solution for taking the water susceptibility in the fatigue test into account in the future.

Acknowledgements Open access funding provided by TU Wien (TUU).

Funding This study was funded by ASFINAG and the nine federation states of Austria.

Compliance with ethical standards

Conflict of interest The authors declare that they have no conflict of interest.

Open Access This article is distributed under the terms of the Creative Commons Attribution 4.0 International License (<http://creativecommons.org/licenses/by/4.0/>), which permits unrestricted use, distribution, and reproduction in any medium, provided you give appropriate credit to the original author(s) and the source, provide a link to the Creative Commons license, and indicate if changes were made.

References

- Smith BJ, Hesp SAM (2000) Crack pinning in asphalt mastic and concrete—regular fatigue studies. *Asph Binders* 2000(1728):75–81
- Kim YR, Little DN, Song IJ (1832) Effect of mineral fillers on fatigue resistance and fundamental material characteristics—mechanistic evaluation. *Bitum Paving Mix* 2003(2003):1–8
- Martono W, Bahia HU, D'Angelo J (2007) Effect of testing geometry on measuring fatigue of asphalt binders and mastics. *J Mater Civ Eng* 19(9):746–752
- CEN (2012) EN 12697-24: bituminous mixtures—test methods for hot mix asphalt—part 24: resistance to fatigue. Brussels
- Van Rompu J et al (2012) New fatigue test on bituminous binders: experimental results and modeling. *Constr Build Mater* 37:197–208
- Di Benedetto H, Nguyen QT, Sauzéat C (2011) Nonlinearity, heating, fatigue and thixotropy during cyclic loading of asphalt mixtures. *Road Mater Pavement Des* 12(1):129–158
- Van Rompu J et al (2009) New fatigue test on bituminous binders and mastics using an annular shear rheometer prototype and waves propagation. *Adv Test Charact Bitum Mater* 1 and 2:69–79
- Delaporte B et al (2008) New procedure to evaluate fatigue of bituminous mastics using an annular shear rheometer prototype. *Pavement cracking: mechanisms, modeling, detection, testing and case histories*, pp 457–467
- Kim Y-R, Lee H-J (2003) Evaluation of the effect of aging on mechanical and fatigue properties of sand asphalt mixtures. *KSCE J Civ Eng* 7(4):389–398
- Kim YR, Little DN, Lytton RL (2003) Fatigue and healing characterization of asphalt mixtures. *J Mater Civ Eng* 15(1):75–83
- Kim YR, Little DN, Lytton RL (2002) Use of dynamic mechanical analysis (DMA) to evaluate the fatigue and healing potential of asphalt binders in sand asphalt mixtures. *J Assoc Asphalt Paving Technol* 71:176–206



12. Taylor R, Airey G (2008) Influence of surface interactions between bitumen and mineral fillers on the rheology of bitumen-filler mastics. In Efficient transportation and pavement systems: characterization, mechanisms, simulation, and modeling. 453 p
13. Cardone F et al (2015) Influence of mineral fillers on the rheological response of polymer-modified bitumens and mastics. *J Traffic Transp Eng (Engl Ed)* 2(6):373–381
14. Ameri M et al (2017) Fatigue performance evaluation of modified asphalt binder using of dissipated energy approach. *Constr Build Mater* 136:184–191
15. Mukandila EM, Steyn WJM, Milne TI (2016) Modelling of cohesion and adhesion damage of seal based on dynamic shear rheometer testing. *Int J Pavement Eng* 1–12. <https://doi.org/10.1080/10298436.2016.1208197>
16. Shan L et al (2015) Effect of load control mode on the fatigue performance of asphalt binder. *Mater Struct* 49(4):1391–1402
17. Santagata E et al (2015) Fatigue properties of bituminous binders reinforced with carbon nanotubes. *Int J Pavement Eng* 16(1):80–90
18. Liao M-C, Airey G, Chen J-S (2013) Mechanical properties of filler-asphalt mastics. *Int J Pavement Res Technol* 6(5):576–581
19. Hintz C, Bahia H (2013) Understanding mechanisms leading to asphalt binder fatigue in the dynamic shear rheometer. *Road Mater Pavement Des* 14:231–251
20. Stimilli A et al (2012) Effect of healing on fatigue law parameters of asphalt binders. *Transp Res Rec* 2293:96–105
21. Mo LT et al (2012) Research of bituminous mortar fatigue test method based on dynamic shear rheometer. *J Test Eval* 40(1):84–90
22. Liao MC, Chen JS, Tsou KW (2012) Fatigue characteristics of bitumen-filler mastics and asphalt mixtures. *J Mater Civ Eng* 24(7):916–923
23. Soenen H, de La Roche C, Redelius P (2011) Fatigue behaviour of bituminous materials: from binders to mixes. *Road Mater Pavement Des* 4(1):7–27
24. Shen S et al (2011) A dissipated energy approach to fatigue evaluation. *Road Mater Pavement Des* 7(1):47–69
25. Shan LY et al (2011) Separation of thixotropy from fatigue process of asphalt binder. *Transp Res Rec* 2207:89–98
26. Ortiz OJR, Jimenez FEP (2011) Studying asphalt binder fatigue pattern by using a dynamic shear rheometer. *Ing E Investig* 31(1):47–55
27. Liu G et al (2011) Influence of organo-montmorillonites on fatigue properties of bitumen and mortar. *Int J Fatigue* 33(12):1574–1582
28. Shen SH, Chiu HM, Huang H (2010) Characterization of fatigue and healing in asphalt binders. *J Mater Civ Eng* 22(9):846–852
29. Shan L et al (2010) Application of thixotropy to analyze fatigue and healing characteristics of asphalt binder. *Transp Res Rec J Transp Res Board* 2179:85–92
30. Planche J-P et al (2004) Evaluation of fatigue properties of bituminous binders. *Mater Struct* 37(5):356–359
31. Bonnetti K, Nam K, Bahia H (2002) Measuring and defining fatigue behavior of asphalt binders. *Transp Res Rec J Transp Res Board* 1810:33–43
32. Anderson DA et al (2001) Evaluation of fatigue criteria for asphalt binders. *Asph Binders* 2001(1766):48–56
33. Bahia HU et al (1999) Non-linear viscoelastic and fatigue properties of asphalt binders. *J Assoc Asph Paving Technol* 68(1999):1–34
34. CEN (2012) EN 14770: bitumen and bituminous binders—determination of complex shear modulus and phase angle—dynamic shear rheometer (DSR). Brussels
35. CEN (2012) EN 14771: bitumen and bituminous binders—determination of the flexural creep stiffness—bending beam rheometer (BBR). Brussels
36. AASHTO (2010) AASHTO M 320-10: standard specification for performance-graded asphalt binder. American Association of State and Highway Transportation Officials, Washington
37. CEN (2016) EN 1426: bitumen and bituminous binders—determination of needle penetration. Brussels
38. CEN (2015) EN 1427: bitumen and bituminous binders—determination of the softening point—ring and ball method. Brussels
39. CEN (2015) EN 12593: bitumen and bituminous binders—determination of the Fraass breaking point. Brussels